Journal of Neuroscience Methods 176 (2009) 254–262

Contents lists available at ScienceDirect

Journal of Neuroscience Methods

journal homepage: www.elsevier.com/locate/jneumeth

Measuring early pre-symptomatic changes in locomotion of SOD1-G93A rats—A rodent model of amyotrophic lateral sclerosis

Wenlong Tang[a], Uri Tasch[a,*], Nagaraj K. Neerchal[b], Liang Zhu[a], Paul Yarowsky[c]

[a] Department of Mechanical Engineering, University of Maryland, Baltimore County, Baltimore, MD 21250, United States
[b] Department of Mathematics and Statistics, University of Maryland, Baltimore County, Baltimore, MD 21250, United States
[c] Department of Pharmacology and Experimental Therapeutics, University of Maryland School of Medicine and the Veterans Administration, Baltimore, MD 21201, United States

ARTICLE INFO

Article history:
Received 10 July 2008
Received in revised form 20 August 2008
Accepted 21 August 2008

Keywords:
SOD1-G93A mutants
ALS
Locomotion
Logistic regression

ABSTRACT

A locomotion analysis system for laboratory rats is presented. The system produces locomotion parameters (LPs) in 4 different domains: force, space, time and frequency. Video images of the walking rats are used to associate the system signals with individual limbs. Numerous LPs can be derived for every test run when the rat walks through the system on the way to sweets and a personal toy placed at the exit. This manuscript demonstrates that in order to differentiate SOD1-G93A mutant rat, a model of amyotrophic lateral sclerosis (ALS), from a Sprague Dawley (SD) control rat at a pre-symptomatic stage, one has only to use 8 key parameters. These 8 parameters are the bio-markers of ALS. The spline-based transformed values of these parameters are used as explanatory variables of a logistic regression model. This model predicts the probability that the examined rat belongs to the SOD1-G93A group. The model differentiates faultlessly between the SOD1 and control groups from the very first time the rats walked through the system at 51 days old. This system provides a new paradigm for ALS diagnosis, and it can have a significant impact on the development of new therapeutic procedures for ALS. The methodology presented in this manuscript can further address the development and validation of therapeutic procedures for other neurological diseases that affect locomotion.

1. Introduction

Amyotrophic lateral sclerosis (ALS) is a serious neurodegenerative disease that affects almost selectively motor neurons (Galan et al., 2007). ALS is very difficult to diagnose in the early stages because the symptoms are similar to those of other, often treatable, neuromuscular disorders where neurodegeneration does not occur. The diagnosis of ALS is usually based on a complete neurological examination and various clinical tests. Since the initial symptoms of ALS are unremarkable, the disease is often undetected in its early stages. However, as more motor neurons fail, the muscles controlled by them stop functioning normally. Eventually, the muscles weaken and become paralyzed and, in most cases, a respiratory failure is the cause of death.

At the present time, there is no effective treatment for ALS. This is due in part to the motor neurons' degeneration and the contributions of other cells, known as glia, towards their demise. Current treatments help control the symptoms but they do not stop the progression of the disease or cure it. Furthermore, the search for new therapeutic procedures has been hindered by the lack of early and reliable diagnosis. Early detection of ALS is essential for both identifying appropriate candidate animals for inclusion in the treatment group and monitoring the progress and efficacy of the treatment. Thus, early detection and the ability to assess the progression of the disease are critical for the development of new and effective therapeutic treatments for ALS.

Laboratory animal models have been used to study the progression of ALS in rats and mice. SOD1-G93A rats (Jackson et al., 2002; Howland et al., 2002) have been accepted as animal model for ALS due to their similarities to human ALS symptoms, including muscle weakness, weight loss, chewing reflex, paralysis, and breathing difficulties.

Researchers have investigated motor symptoms that detect ALS early. Kafkafi et al. (2008) reported that a Pattern Array for data mining of movement distinguishes control SD rats from SOD1-G93A mutant rats at pre-symptomatic ages. The former exhibit heavy breaking when moving along an arena wall and turning away from it, whereas the SOD1-G93A mutants fail to exhibit this behavioral pattern. According to Kafkafi et al. (2008), these symptoms

* Corresponding author at: Department of Mechanical Engineering, University of Maryland, Baltimore County, 1000 Hilltop Circle, Baltimore, MD 21250, United States. Tel.: +1 410 455 3305; fax: +1 410 455 1052.
E-mail address: tasch@umbc.edu (U. Tasch).

0165-0270/$ – see front matter © 2008 Elsevier B.V. All rights reserved.
doi:10.1016/j.jneumeth.2008.08.032

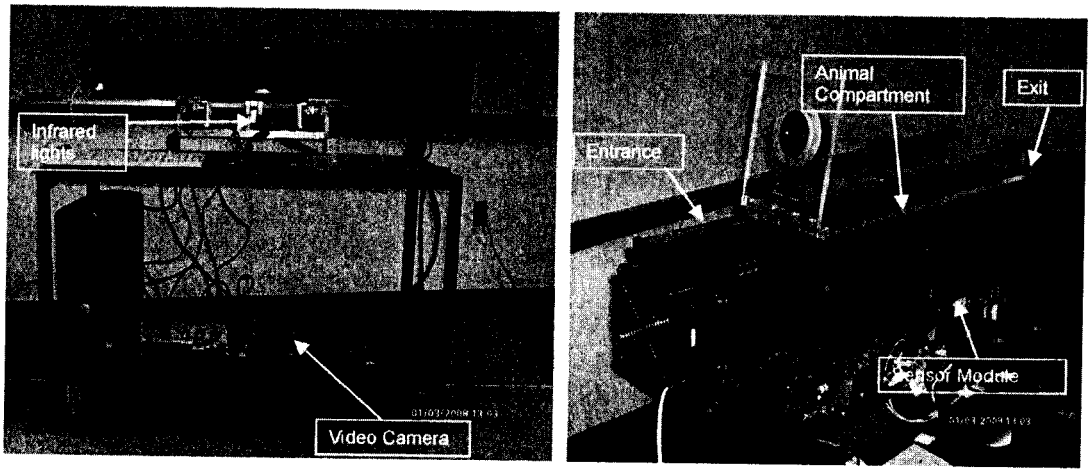

Fig. 1. A locomotion analysis system for rodents. The system measures LPs in 4 domains: force, space, time and frequency. The measured forces are in vertical, longitudinal and transverse directions. A video camera records bottom images of the rat that walks through the system, and through synchronization of the video images and load cell signals, one can recognize the ground reaction forces of each individual limb.

may enable researchers to test therapies that address intervention rather than remediation.

This manuscript describes a quantitative method to diagnose the presence or absence of locomotion dysfunction in a rodent model of ALS. The diagnosis is based on a number of locomotion parameters (LPs) generated at each stride of every limb as the animal walks freely through a narrow passage to get to its individual toy and food placed at the system exit. Using several repeated walks of animals with known disease conditions, we build predictive models for ALS in terms of LPs that have been transformed through spline transformations (Liu et al., 2008). The transformed LPs are used as explanatory variables of a logistic regression model for the probability that the examined rat belongs to the SOD1-G93A mutant group.

The locomotion analysis system, described in this manuscript, can measure numerous LPs for every test run. In this manuscript 110 LPs per animal per run are evaluated for their ability to identify the presence of the disease. For each LP, we explore a nonlinear transformation based on spline functions, which best predict the presence of ALS. It is demonstrated that in order to classify SOD1-G93A rats correctly one has to measure only 8 very particular LPs per limb. It turns out that the system is capable of distinguishing between the SOD1 mutants and control SD animals correctly from the very first time the animal crosses the system.

2. Materials and methods

2.1. Design of the locomotion analysis system

The locomotion analysis system, introduced in Tasch et al. (2008), underwent several enhancements. First, it was mounted on a steel cart to improve its mobility (Fig. 1); also two highly sensitive load cells (Transducer Techniques, 150 g #206757) were mounted to measure the longitudinal ground reaction forces (GRF), and four standard parallelogram tension/compression load cells (Omega LCLB-2) were mounted to measure the transverse GRF. Finally, a digital video camera (Sony, DMK 31BF03) was mounted on the base shelf to record the bottom view of the walking rats. To con-

Table 1
Definitions of the 20 LMV evaluated in this manuscript.

No.	Variable	Units	Definition
1	Fz_{max}	Non-dimensional	Maximum value of the vertical GRF component of a selected limb
2	Stance Time	s	Time duration that a selected limb is in contact with the floor
3	T_Fz_{max}	Non-dimensional	Time of Fz_{max} normalized by the Stance Time of a selected limb
4	Fz_{mean}	Non-dimensional	The mean value of the vertical GRF component of a selected limb ($\int_{S.Time} Fz\,dt$/Stance Time)
5	Fz_{ω}	s^{-1}	The Fourier transform of Fz summed over the first 50 Hz for a selected limb ($\int_{50} Fz\,d\omega$)
6	Stride	Non-dimensional	Stride length of a selected limb calculated as the difference between two consecutive contact positions; the contact positions are normalized by the floor length, which is 13.25 in.
7	Fy_{max}	Non-dimensional	Maximum value of the longitudinal GRF component of a selected paw
8	T_Fy_{max}	Non-dimensional	Time of Fy_{max} divided by Stance Time
9	Fy_{min}	Non-dimensional	Minimum value of the longitudinal GRF component of a selected paw
10	T_Fy_{min}	Non-dimensional	Time of Fy_{min} divided by Stance Time
11	Fy_{mean}	Non-dimensional	The average value of the longitudinal GRF component of a selected paw [$\int_{S.Time} Fy\,dt$/Stance Time]
12	Fy_{ω}	s^{-1}	The Fourier transform of Fy summed over the first 50 Hz for a selected paw [$\int_{50} Fy\,d\omega$]
13	Fx_{max}	Non-dimensional	Maximum value of the transverse GRF component of a selected paw
14	Fx_{min}	Non-dimensional	Minimum value of the transverse GRF component of a selected paw
15	Fx_{mean}	Non-dimensional	The average value of the transverse GRF component of a selected paw [$\int_{S.Time} Fx\,dt$/Stance Time]
16	FyP	Non-dimensional	The mean value of the propelling (positive) longitudinal force of a selected limb
17	FyB	Non-dimensional	The mean value of the braking (negative) longitudinal force of a selected limb
18	NP	Non-dimensional	The number of samples in which the longitudinal force is propelling (positive in value); the sampling rate is 200 Hz
19	NB	Non-dimensional	The number of samples in which the longitudinal force is braking (negative in value); the sampling rate is 200 Hz
20	NPB	Non-dimensional	The number of times in which the longitudinal force switches sign from braking to propelling and vise versa

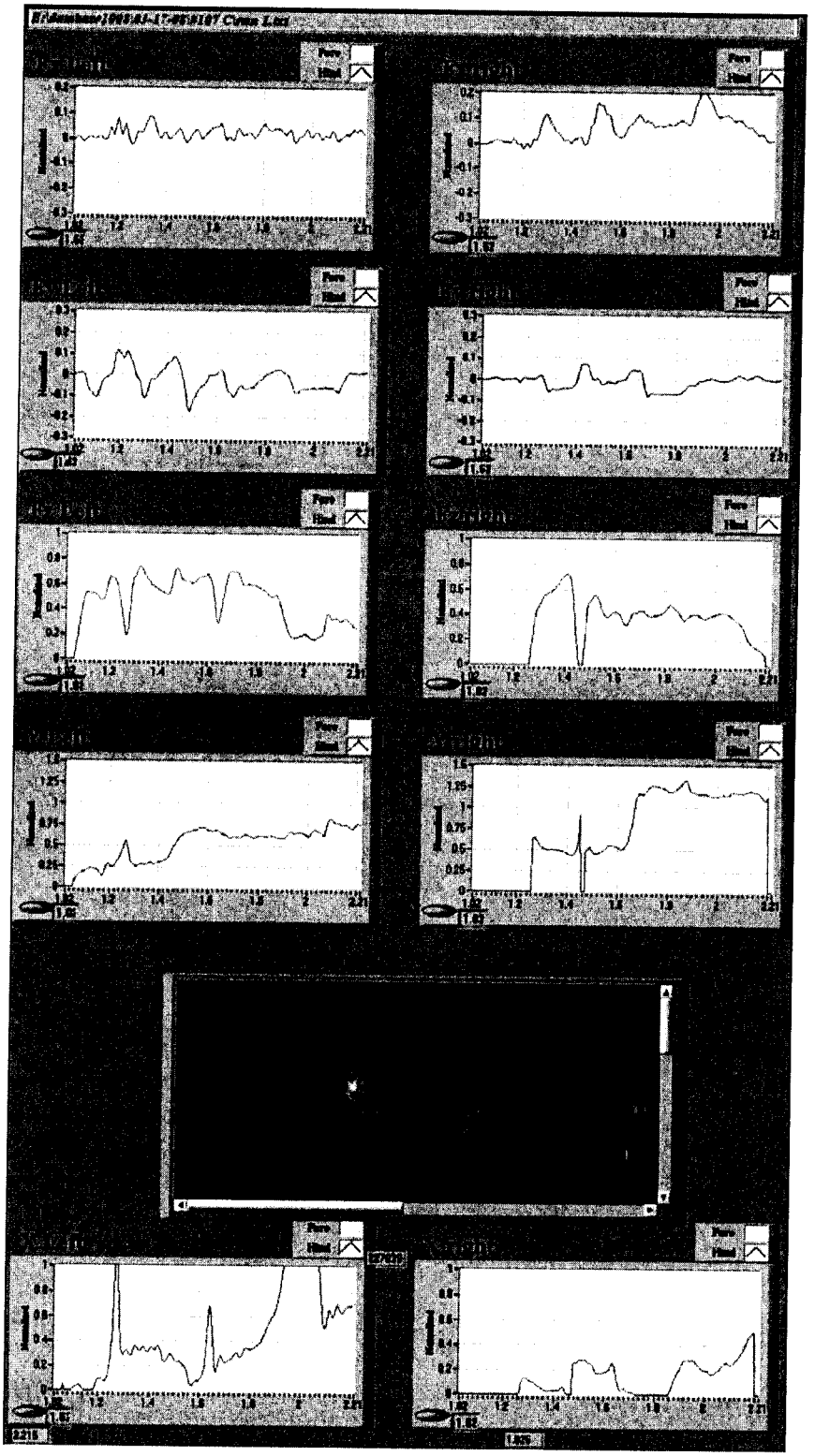

Fig. 2. The outputs generated by the locomotion analysis system in a typical test run. The signatures of the left and right limbs are depicted on the left and right sides, respectively. The transverse (Fx), longitudinal (Fy), and vertical (Fz) are normalized with respect to the rat's body weight and plotted as a function of time (s). The longitudinal (*Y*) and transverse (*X*) limb positions are normalized with respect to the length and width of the floor plates, respectively. A video image of the bottom of the rat is also recorded.

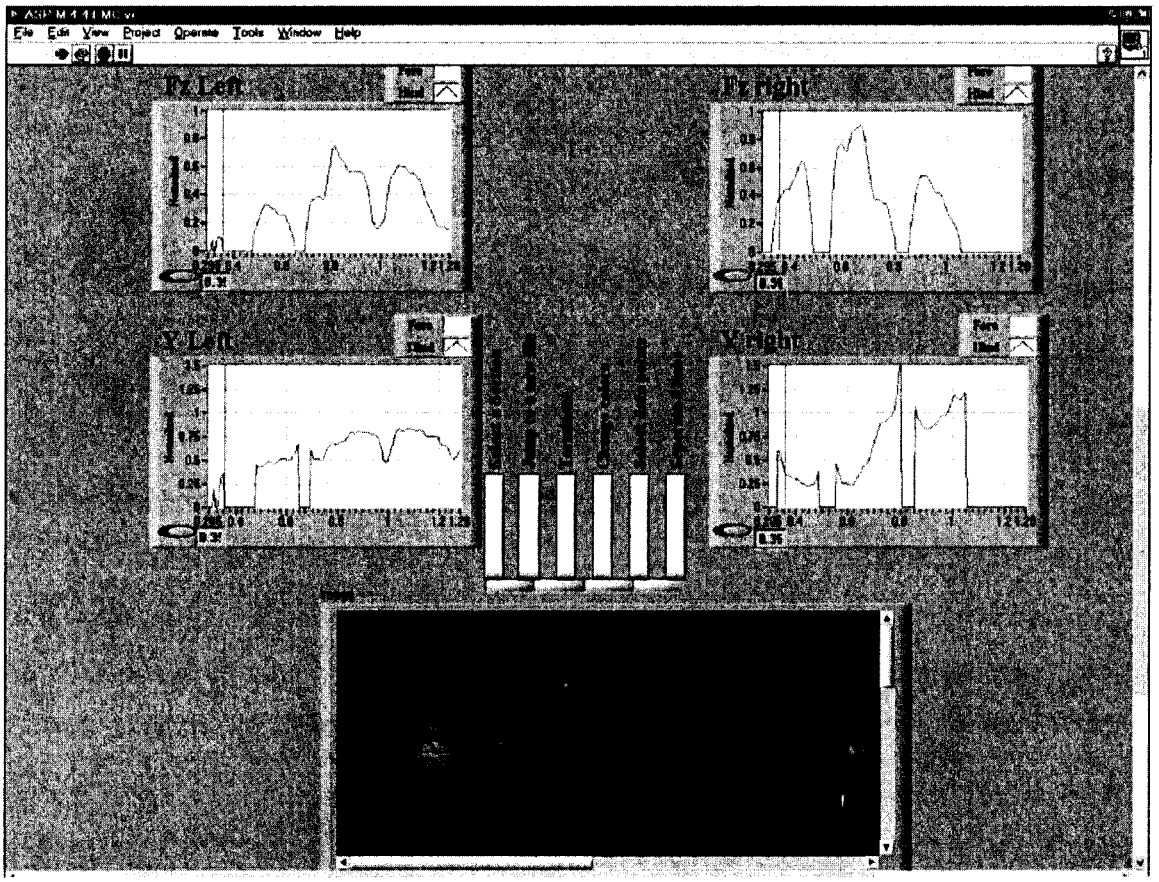

Fig. 3. To associate a load cell signature with a limb the computer mouse is placed on a selected signature (vertical marker) and the most recent video image is displayed. The load cell signature on the right from 0.33 to 0.49 s is associated with the right fore limb.

trol the lighting two arrays of infrared LEDs were also mounted (see Fig. 1). These enhancements resulted in a locomotion system that records video images as well as vertical, longitudinal, and transverse GRF and spatial (longitudinal and transverse) limb positions of walking rats. The load cell data was recorded at a rate of 200 Hz and the video recording at 30 fps.

2.2. Obtaining gait measurements

4 SOD1-G93A mutant and 4 Sprague–Dawley (SD) control rats from Taconic Laboratory (Germantown, NY) participated in the study. The rats were all males and 4 weeks old upon their arrival on 7 January, 2008. Each rat was housed in a separate cage with inversed darkness/lighting cycle and food and water *ad libitum*. After weighing the animal it was placed at the system entrance, the gate was opened, and the rat crossed the system moving toward its individual cylindrical toy and a treat of condensed milk, both of which were placed at the system exit. This procedure was repeated up to three times for each rat on a single day. After a period of 10 days of training and adaptation to the system, each animal was tested twice per week and data was recorded from 30 January, when the rats were 51 days old, through 24 March, 2008 or until the rats were 105 days of age. The database contained 163 test runs, where 96 records were from SOD1 mutants and 67 from control SD rats. At the end of the experiment, rats were euthanized by sodium pentobarbital (150 mg/kg IP). Our protocol has been approved by the IACUC at the University of Maryland, Baltimore County and the University of Maryland, School of Medicine.

2.3. Locomotion parameters (LPs)

From the signals of 14 load cells the values of 20 LPs per limb were evaluated for the left fore (LF), right fore (RF), left hind (LH), and right hind (RH) limbs. The 20 LPs, listed in Table 1, are non-dimensional except to Stance Time, Fz_ω, and Fy_ω that have dimensions of s, s^{-1}, and s^{-1}, respectively.

2.4. Logistic regression

In an earlier work we addressed modeling of bovine lameness, and we used logistic regression to evaluate lameness predictions of dairy cattle (Rajkondawar et al., 2002). In the current manuscript, logistic regression models (Hosmer and Lemeshaw, 2000) are used to predict the probability that an examined rat belongs to the SOD1-G93A mutant group in terms of the LPs. This is expressed mathematically as

$$P(\text{a rat} \in \text{SOD1 group}) = \frac{\exp\left(\sum \beta_i \text{LP}_i\right)}{1 + \exp\left(\sum \beta_i \text{LP}_i\right)} \quad (1)$$

where the β_i is the ith coefficient of the logistic regression model and is estimated by appropriate statistical methods. Liu et al. (2008) demonstrated that the accuracy of the predictions of such models is significantly improved when the LPs are transformed via spline transformations. An implementation of these transformations is available in SAS (PROC TRANSREG) (SAS Institute Inc., 2004). The probability that a rat belongs to the SOD1-G93A mutant group is

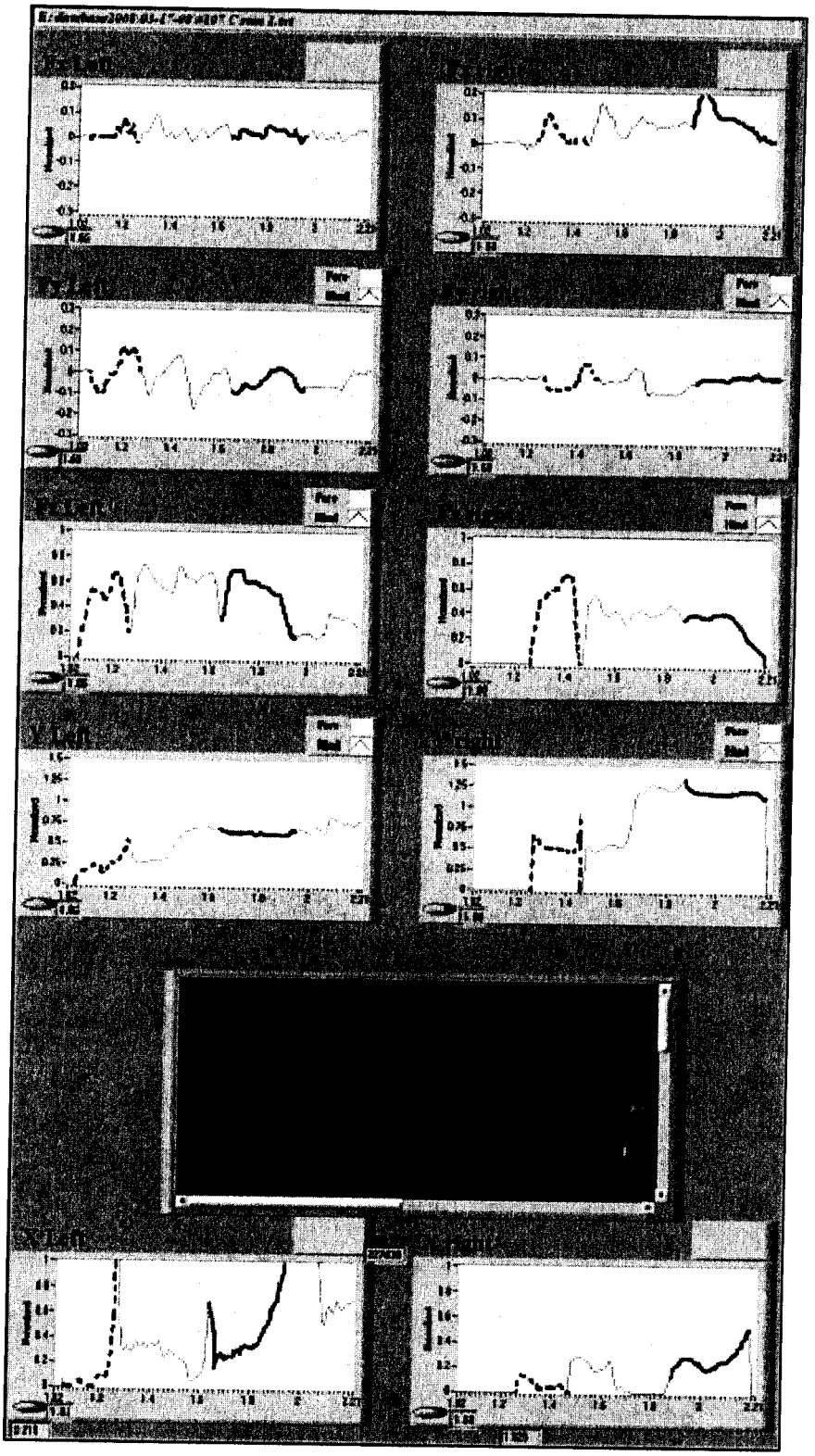

Fig. 4. The load signatures generated by a single limb are identified and following the procedure shown in Fig. 3, the fore and hind limbs are marked with dashed and solid heavy lines, respectively.

Table 2
Definitions of 15 symmetry factors.

No.	Variable	Units	Definition
1	Sym_Fz_{max}	Non-dimensional	Symmetry factor of Fz_{max}
2	Sym_Stance Time	Non-dimensional	Symmetry of Stance Time
3	Sym_T_Fz_{max}	Non-dimensional	Symmetry of T_Fz_{max}
4	Sym_Fz_{mean}	Non-dimensional	Symmetry of Fz_{mean}
5	Sym_Fz_{ω}	Non-dimensional	Symmetry of Fz_{ω}
6	Sym_Stride	Non-dimensional	Symmetry of Stride
7	Sym_Fy_{max}	Non-dimensional	Symmetry of Fy_{max}
8	Sym_T_Fy_{max}	Non-dimensional	Symmetry of T_Fy_{max}
9	Sym_Fy_{min}	Non-dimensional	Symmetry of Fy_{min}
10	Sym_T_Fy_{min}	Non-dimensional	Symmetry of T_Fy_{min}
11	Sym_Fy_{mean}	Non-dimensional	Symmetry of Fy_{mean}
12	Sym_Fy_{ω}	Non-dimensional	Symmetry of Fy_{ω}
13	Sym_Fx_{max}	Non-dimensional	Symmetry of Fx_{max}
14	Sym_Fx_{min}	Non-dimensional	Symmetry of Fx_{min}
15	Sym_Fx_{mean}	Non-dimensional	Symmetry of Fx_{mean}

hence evaluated as:

$$P(\text{a rat} \in \text{SOD1 group}) = \frac{\exp\left(\sum \beta_i \text{TLP}_i\right)}{1 + \exp\left(\sum \beta_i \text{TLP}_i\right)} \quad (2)$$

where TLP_i is the transformed value of LP_i.

2.5. Cross-validation

Leave-one-out (Kohavi, 1995) method of cross-validation was used to evaluate the performance of the derived ALS models. A single test run from the original sample is taken as the validation data, and the remaining test runs are taken as the training data. This procedure is repeated 163 times until every test run in the database is used once as the validation data.

3. Results

A typical output of a single test run is depicted in Fig. 2. These outputs are recorded from an array of fourteen load cells that support the left and right floor plates of the system sensor module, as described in Tasch et al. (2008). Vertical (Fz), longitudinal (Fy), and transverse (Fx) GRF components, as well as longitudinal (Y) and transverse (X) limb positions, are plotted versus time (s) for both left and right floor plates. In addition, bottom images of the walking rat are recorded by a video camera. Fz, Fy, and Fx are normalized with respect to the animal's body weight, and the longitudinal (Y) and transverse (X) limb positions are normalized with respect to the length and width, respectively of the sensor module floors. Thus $Y = 0$ denotes the entrance, and $Y = 1$ denotes the exit, where $X = 0$ denotes the center line and $X = 1$ the far edge (see Fig. 2).

Table 4
Misclassification rate, in percentage, obtained by using a single LP or its associated transform TLP.

Locomotion parameter LP	Misclassification rate of LP (%)	Misclassification rate of TLP (%)
FyB	34.0	18.4
T_Fy_{max}	33.1	20.3
Fy_{max}	40.5	24.5
Fz_{ω}	41.7	25.2
Fz_{mean}	40.5	25.8
Fy_{ω}	37.4	25.8
NP	38.6	25.8
Fx_{max}	41.7	25.8
Fz_{max}	42.3	26.4
FyP	41.2	26.4
T_Fy_{min}	39.3	27.0
Stance Time	36.2	27.6
Fy_{min}	38.7	27.6
Fy_{mean}	36.8	27.6
Stride	40.5	28.2
Fx_{mean}	36.6	28.2
NB	38.6	28.2
Sym_Fx_{min}	41.1	28.8
T_Fz_{max}	40.5	28.8
Sym_T_Fy_{max}	41.3	29.5
Sym_Fx_{max}	41.7	31.9
Sym_Stance Time	38.0	32.5
Fx_{min}	42.3	32.5
Fy_{ω}	40.5	33.1
Sym_T_Fz_{max}	41.5	33.7
Sym_Fy_{max}	41.1	33.7
NPB	41.8	33.7
Sym_Fz_{mean}	37.4	34.4
Sym_Fz_{max}	42.3	35.0
Sym_T_Fy_{min}	42.0	35.0
Sym_Fy_{mean}	40.5	35.0
Sym_Fz_{ω}	36.4	35.6
Sym_Fx_{mean}	38.7	35.6
Sym_Fy_{min}	42.0	38.7
Sym_Stride	41.7	39.9

Table 3
Numerical values of the 20 measured LPs for each (LF. RF. LH, RH) limbs and the 15 symmetry factors for fore and hind limbs for a control rat #107.

Locomotion parameter (LP)	LF	RF	LH	RH	Sym_LP_F	Sym_LP_H
Fz_{max}	0.7398	0.8116	0.7357	0.7254	−0.046	0.007
Stance Time (s)	0.1550	0.1400	0.2900	0.1750	0.051	0.247
T_Fz_{max}	0.3226	0.7500	0.2241	0.2857	−0.398	−0.121
Fz_{mean}	0.5288	0.5260	0.4221	0.3918	0.003	0.037
Fz_{ω} (s^{-1})	0.5326	0.5280	0.5194	0.4605	0.004	0.060
Stride	0.3463	0.7202	0.4133	0.6818	−0.351	−0.245
Fy_{max}	0.1517	0.3986	0.0178	0.3771	−0.449	−0.910
T_Fy_{max}	0.8710	0.1786	0.5172	0.4571	0.660	0.062
Fy_{min}	−0.4292	−0.1286	−0.1237	−0.0805	0.539	0.211
T_Fy_{min}	0.2258	0.5714	0.1207	0.2857	−0.434	−0.406
Fy_{mean}	−0.1504	0.0948	−0.0384	0.0660	4.411	−3.779
Fy_{ω} (s^{-1})	0.2769	0.2621	0.0842	0.2377	0.027	−0.477
Fx_{max}	0.0493	0.1102	0.1040	0.1944	−0.381	−0.303
Fx_{min}	−0.0462	−0.0610	0.0231	0.0163	−0.138	0.175
Fx_{mean}	−0.0005	0.0201	0.0661	0.1093	−1.048	−0.246
FyP	0.0829	0.0111	0.0188	0.0029		
FyB	−0.1936	−0.0440	−0.7466	−0.1794		
NP	5	6	22	23		
NB	27	53	7	13		
NPB	5	2	5	1		

This data is run #1 recorded on 21 March, 2008 and the rat was 102 days old. Except for Stance Time, Fz_{ω}, and Fy_{ω} all variables are non-dimensional.

At any time the left and right floors can be in contact with one, two, or no limbs. When a single limb is in contact with the floor plate, we synchronize the load cell outputs that are recorded at 200 Hz, with the most recent video image recorded at 30 fps. This enables us to verify the association between an individual limb and a recorded force signature. Fig. 3 demonstrates that the output signatures of the right floor plate during the time period of 0.33–0.49 s are generated when the right fore limb is in contact with the floor. Similarly, one can associate the other limbs with the load cell signals they generate. Thus each fore and hind limb is designated with dashed and solid lines, respectively (Fig. 4). This enables one to calculate numerous LPs that characterize the locomotion of a rat through each limb for every test run.

Table 1 lists the 20 LPs that were evaluated for every limb in this manuscript. The list includes gait parameters that characterize the vertical (Fz), longitudinal (Fy) and transverse (Fx) forces, as well as parameters that are associated with time, stride, and frequency (Fz_ω and Fy_ω). In addition to the 20 LPs, listed in Table 1, we derived parameters that capture symmetry between the left and right sides of the animal. This is based on the hypothesis that control rats exhibit left/right LP symmetry. Symmetry of any LP is defined as

$$\text{Sym\_LP} = \frac{\text{LP}_{\text{left}} - \text{LP}_{\text{right}}}{\text{LP}_{\text{left}} + \text{LP}_{\text{right}}}. \quad (3)$$

Eq. (3) can be applied to any of the 20 LPs listed in Table 1. Symmetry can be evaluated for the hind (Sym_LP_H) or the fore (Sym_LP_F) limbs. The symmetry factors, listed in Table 2, were evaluated for the fore and hind limbs in this manuscript.

The 20 LPs, listed in Table 1, were evaluated for LF, RF, LH, and RH limbs and the symmetry factors, listed in Table 2, were evaluated for the forelimbs and hind-limbs for every test run of the 4 control and 4 SOD1-G93A rats. A typical data for a single test run contained values of 110 parameters, as depicted in Table 3.

In an effort to rank the 20 LPs and 15 symmetry factors, we examined the effectiveness of each individual parameter, to classify correctly the rats into the SOD1-G93A mutant and control groups. Using previous modeling experience, we transformed the LPs by following the procedures introduced in Liu et al. (2008), and Neerchal and Tasch (2008). The misclassification rate improved remarkably when transformed LP (TLP) was used (see Table 4). Therefore, we explored the idea of transforming the LP variables using nonlinear transformations (TLP) to improve the prediction performance of the model. One such family of nonlinear transformations is obtained by expanding each LP in terms of a spline basis (Schumaker, 2007). The misclassification performance of each

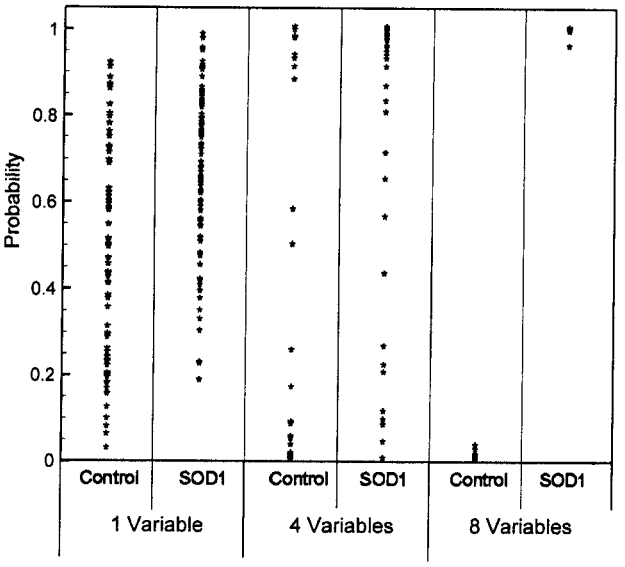

Fig. 5. The range of predicting probabilities that the examined rat belongs to the SOD1-G93A group. Note large spread and big overlap between the control and SOD1-G93A groups when 1 variable is used. When 4 variables are used the overlap between the two groups somewhat shrinks, nevertheless when a 8-variable model is used there is a complete separation between the control and the SOD1 groups. This complete separation enables us to classify the rats correctly in each and every test run.

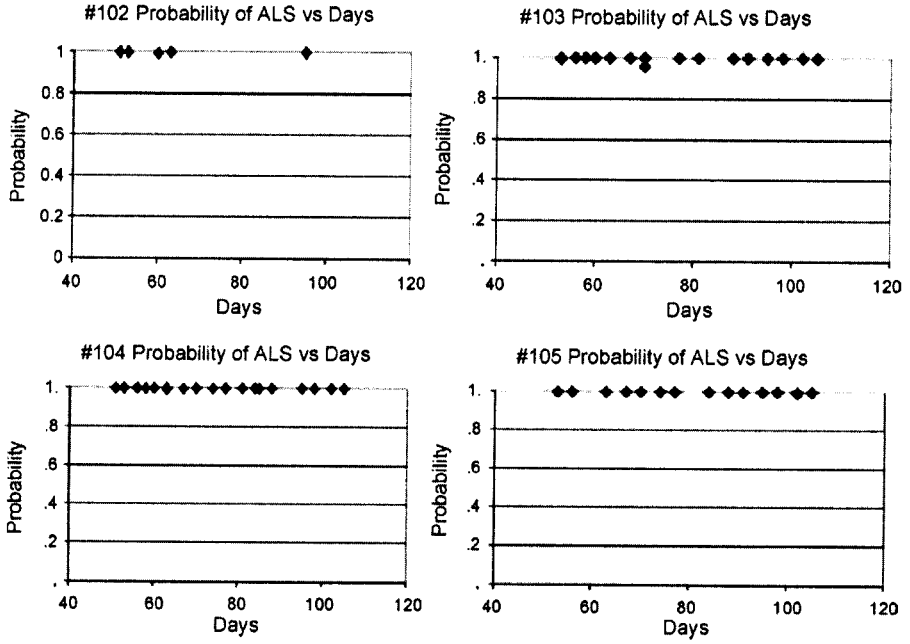

Fig. 6. The probabilities that a SOD1-G93A mutant belongs to the SOD1-G93A group versus the rats' age (D). Note that for every run the probability is above 0.95 for each of the 4 SOD1-G93A rats. Further, note that the rats walk at their own pace and some rats are more active than others.

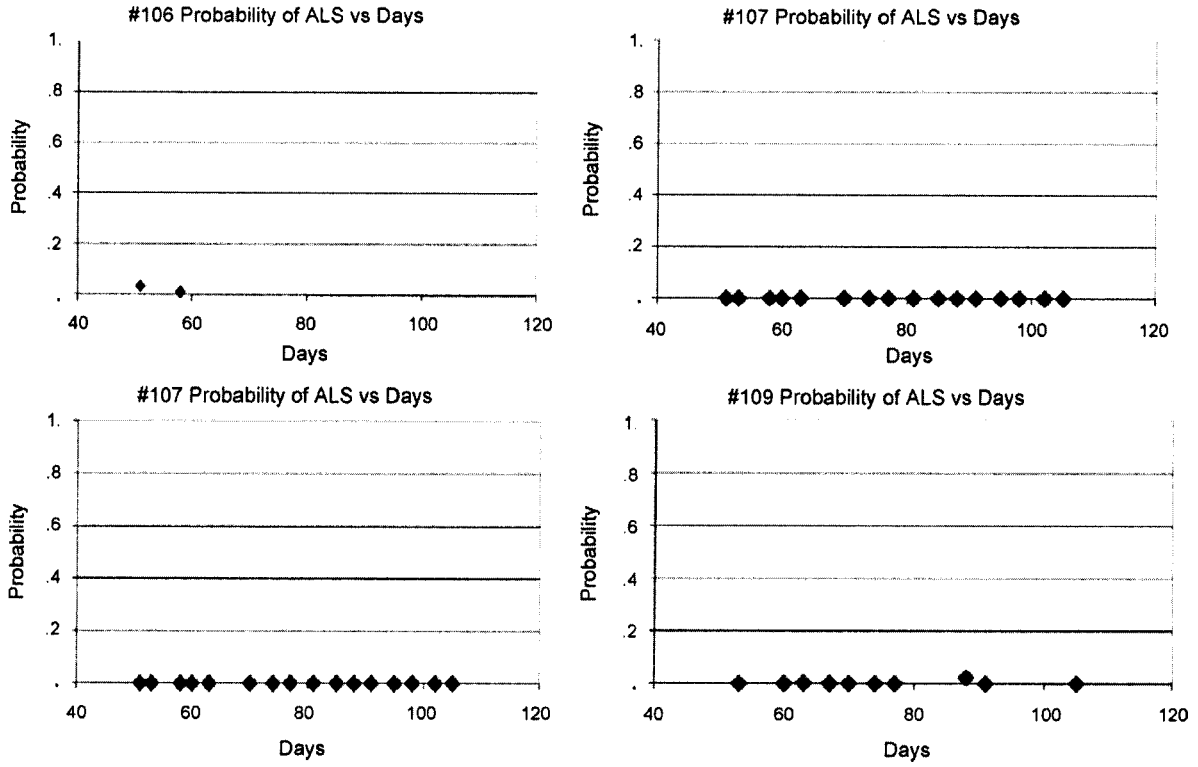

Fig. 7. The probabilities that a control rat belongs to the SOD1-G93A group versus the rats' age (D). Note that for every run the probability is below 0.05 for each of the 4 control rats. Furthermore note that the rats walk at their own pace and will and some rats are more active than others.

individual TLP ranged from 18.4 to 39.9%, where FyB had the best performance, and the symmetry factor of the stride (Sym_Stride) had the worst (see Table 4).

Lastly, when the logistic regression model is based on the transformed values of the top 8 variables listed in Table 4 (FyB, T_Fy_{max}, Fy_{max}, Fz_{ω}, Fz_{mean}, Fy_{ω}, NP, and Fx_{max}), the range of probabilities that a control rat belongs to the SOD1-G93A mutant group is from 0.000 to 0.033, and the range of probabilities that an SOD1-G93A mutant belongs to the SOD1 group is from 0.957 to 1.000 (see Fig. 5). Hence, the 8-variable model has no overlap between the SOD1-G93A mutant and the control groups, and its performance turns out to be excellent from the very first test run of the 4 SOD1-G93A mutants (see Fig. 6) and 4 control SD rats (see Fig. 7).

4. Discussion

This manuscript demonstrates that a logistic regression model with the "proper" explanatory locomotion variables can differentiate between SOD1-G93A mutant and control SD rats from the very first time the examined rats cross a locomotion analysis system, and the resultant classification is excellent. The ability to diagnose neurological diseases early will allow researchers to test intervention therapies and hopefully to find therapeutics that are neuroprotective and/or neurorestorative for serious diseases that are currently incurable. The selection of the number of LPs used to construct a logistic regression model was based on the misclassification performance of each individual variable.

Sweets (condensed milk) and individual cylindrical toys that are placed at the exit platform were used to encourage the rats, in the current system design, to walk through the system. Rats walk through the system at their own pace and will. This explains the discrepancies in the number of test runs for different rats. It is apparent that rats #102 and #106 do not walk as often as their test mates rats #103, #104, #105, #107, #108, or #109 (see Figs. 6 and 7).

In this manuscript we examined 4 SOD1-G93A mutant and 4 SD control rats. Obviously, the database consists of several repeated observations. It is well known that repeated observations from the same rat may be correlated. Correlated observations usually do not affect the predictions adversely, but they cause the corresponding prediction errors to be under-estimated. The current study demonstrates the feasibility of the approach however a much larger study with larger number of rats is needed. We plan to use the results of this manuscript as a basis for a power study to investigate sample size issues. Obviously, one needs to repeat the experiments with larger populations. Nevertheless, the analysis presented here is not based on visualization of gait abnormalities, as all the SOD1-G93A animals were pre-symptomatic. It has been demonstrated that the earliest change in locomotion is at the neuromuscular junction where there is a process of denervation and re-innervation occurring before any changes in the number of lower motor neurons have occurred (Fischer et al., 2004).

It can be hypothesized that various other neurological disorders that affect gait, such as Parkinson disease, Huntington disease, and Multiple Sclerosis, could also be diagnosed in laboratory animal models using the same methodology. The key will be to find the "proper" LPs that constitute biomarkers of the disease one investigates. Furthermore, various pattern recognition strategies can be employed to develop diagnostic tools for other neurological diseases.

Acknowledgments

The financial support provided by the Laboratory of Neurosciences at NIA and the technical support of Dr. Donald K. Ingram

are gratefully acknowledged. Support was also provided by the Veterans Administration (PY). Furthermore, the support of the staff of the animal facility at UMBC, Ms. Kirsty L. Carrihill-Knoll and Ms. Rosie Mills is greatly appreciated.

Appendix A. Supplementary data

Supplementary data associated with this article can be found, in the online version, at doi:10.1016/j.jneumeth.2008.08.032.

References

Fischer LR, Culver DG, Tennant P, Davis AA, Wang M, Castellano-Sanchez A, et al. Amyotrophic lateral sclerosis is a distal axonopathy: evidence in mice and man. Exp Neurol 2004;185:232–40.

Galan L, Vela A, Guerrero A, Barcia JA, Garcia-Verdugo JM, Matias-Guiu J. Experimental models of amyotrophic lateral sclerosis. J Neurol 2007;22(6):381–8.

Hosmer DW, Lemeshaw S. Applied logistic regression. New York: John Wiley and Sons, Inc; 2000.

Howland DS, Liu J, She Y, Goad B, Maragakis NJ, Kim B, et al. Focal loss of the glutamate transporter EAAT2 in a transgenic rat model of SOD1 mutant-mediated amyotrophic lateral sclerosis (ALS). Proc Natl Acad Sci 2002;5(99(3)):1604–9.

Jackson M, Ganel R, Rothstein JD. Models of amyotrophic lateral sclerosis. Curr Protoc Neurosci 2002;9 [Unit 9.13].

Kafkafi N, Yekutieli D, Yarowsky P, Elmer GI. Data mining in a behavioral test detects early symptoms in a model of amyotrophic lateral sclerosis. Behav Neurosci 2008;122:777–87.

Kohavi R. A study of cross-validation and bootstrap for accuracy estimation and model selection. In: International Joint Conference on Artificial Intelligence; 1995.

Liu J, Dyer RM, Neerchal NK, Rajkondawar PG, Tasch U. Enhancing the predictions accuracy of bovine lameness models through nonlinear transformations of the limb movement variables. In: Proceedings of the 15th International Symposium on Lameness in Ruminants; 2008.

Neerchal NK, Tasch U. Enhancing model prediction accuracy by using spline transformations. Pending patent application; 2008.

Rajkondawar PG, Lefcourt AM, Neerchal NK, Dyer RM, Varner MA, Erez B, et al. The development of an objective lameness scoring system for dairy herds: pilot study. Trans ASAE 2002;45:1123–5.

SAS Institute Inc. SAS/STAT 9.1 user's guide. Cary, NC: SAS Institute, Inc; 2004.

Schumaker LL. Spline functions: basic theory. 3rd ed. Cambridge, UK: Cambridge University Press; 2007.

Tasch U, Moubarak P, Tang W, Zhu L, Lovering RM, Roche J, et al. An instrument that simultaneously measures spatial gait parameters and ground reaction forces of locomoting rats. In: Proceedings of the 9th biennial ASME conference on engineering systems design and analysis. ESDA08; 2008.